A Journal of the Gesellschaft Deutscher Chemiker

Angewandte International Edition

GDCh

Chemie

www.angewandte.org

Accepted Article

Title: Graphdiyne:A New Structure of Fluorescent Quantum Dots

Authors: Huibiao Liu, Jie Guo, Mengyu Guo, Fuhui Wang, Weiyue Jin, Chunying Chen, and Yuliang Li

To be cited as: *Angew. Chem. Int. Ed.* 10.1002/anie.202006891

Link to VoR: https://doi.org/10.1002/anie.202006891

WILEY-VCH

10.1002/anie.202006891

WILEY-VCH

Graphdiyne：A New Structure of Fluorescent Quantum Dots

Jie Guo, Mengyu Guo, Fuhui Wang, Weiyue Jin, Chunying Chen, Huibiao Liu*, Yuliang Li

Abstract: Graphdiyne (GDY) as an emerging two-dimensional carbon allotrope exhibits excellent performance in energy chemistry, catalytic chemistry, optoelectronics, electronics, etc. due to the unique structure combines sp- and sp^2 hybrid carbon network. However, the poor solubility of pristine GDY is the major obstacle to its applications in many fields. Herein, we propose a facile strategy to control the preparation of graphdiyne quantum dots (GDY-Py QDs), in which pyrene groups are covalently linked to GDY by Sonogashira cross-coupling reaction. The as-prepared GDY-Py QDs with average diameter of about 3 ± 0.1 nm show superior dispersibility in many organic solvents and water. The GDY-Py QDs display not only brightly fluorescent with a high relative quantum yield (QY) of 42.82%, but also well-behaved as contrast agents in cell-imaging. The GDY-Py QDs are bestowed with high stability and non-cytotoxicity and exhibit long fluorescent time, which could offer great potential in optical imaging and biomedical application.

Graphdiyne (GDY), as a new generation of two-dimensional carbon allotrope with a unique combination of sp- and sp^2-hybridized π-conjugated carbon network, gives rise to the excellent performance in the fields of separation,[1] sensing,[2] catalysis,[3] electronics,[4] and energy storage/conversion[5] due to its uniformly distributed pores, high electrical conductivity, tunable bandgap, and broad absorption. However, Whether it is a powder or a film, the pristine GDY are difficult to disperse in many solvents including organic solvents and water. The solubility of graphdiyne in solvents hinders its wider application. Therefore, expanding the efficient utilization of GDY in multiple fields to obtain soluble GDY is an important challenge. Recently, our group reported method to prepare water soluble oxidation of GDY through oxide reaction.[6] But the strong oxidant (concentrated sulfuric acid) brings the uncontrollable oxidation as well as the destruction of the partial skeleton in GDY. We have recently prepared graphdiyne derivatives with good solubility in organic solvents by click reaction.[7] The soluble graphdiyne maintains the skeleton and intrinsic nature of graphdiyne. Although the as-prepared graphdiyne is easy to be fabricated uniform film, but it is impossible to succeed for the synthetic highly fluorescent graphdiyne by this method, due to the fluorescence quenching of triazole. Novel structures of graphdiynes with strong fluorescence have the potential to lead to the emergence of new properties, new knowledge and new science. Therefore, exploring new optical properties and applications of GDY-QDs in sensors and biology, etc., has great attracting and scientific significance.

The chemically modified graphdiyne to prepare uniform film without functional groups inspired us to synthesis functional GDY-QDs for more potential application of graphdiyne. With functional chromophore groups, pyrene and its derivatives are usually chosen to boom the fluorescence of functional molecules in cells within extra helps of their chemical stability, high quantum yield (QY), and excellent cell permeability.[8]

Herein, we have synthesized GDY-Py quantum dots (QDs) via Sonogashira cross-coupling reaction, in which 1-bromopyrene (1-BrPy) were conjugated connected with GDY. The GDY-Py QDs have good dispersion in many organic solvents and water. The as-synthesized GDY-Py QDs exhibit an excitation-independent emission with a relative QY of 42.82% superior to most carbon quantum dots[9] and pyrene derivatives,[10] due to the conjugated structure of GDY-Py QDs, which is conducive to improving the electron transfer efficiency between GDY and pyrene. The GDY-Py QDs can be used for imaging cells due to the wide band absorption and enhanced fluorescence properties. The results display that GDY-Py QDs are high photo-stability, very safety for cells and great biocompatibility, which indicates that GDY-Py QDs will be an outstanding candidate for bioimaging.

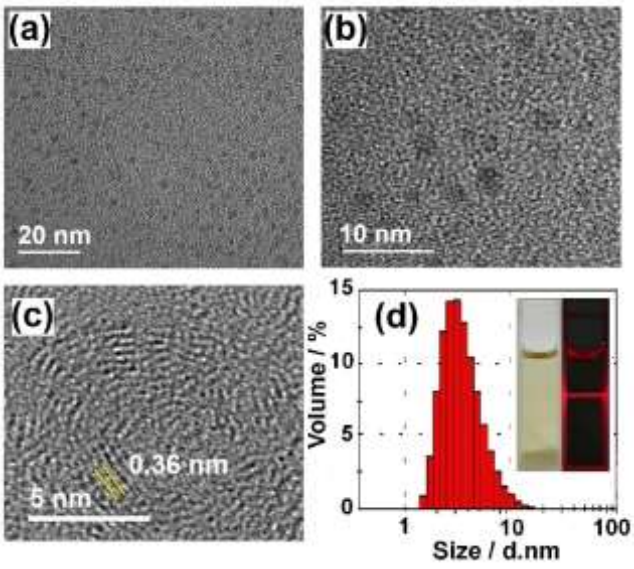

Figure 1. (a), (b) TEM images of the as-prepared GDY-Py QDs. (c) HRTEM image of an individual GDY-Py QDs. (d) The volume-weighted size distribution of GDY-Py QDs dispersion (Insert: photograph and Tyndall phenomenon of GDY-Py QDs in DMF).

Transmission electron microscope (TEM) was used to determine the morphology of the GDY-Py QDs. As shown in Figure 1a and 1b, that these GDY-Py QDs are very uniform with sizes of ca. 3 nm without aggregation. For comparison, the

[a] J. Guo, F. Wang, W. Jin, Prof. H. Liu, Prof. Y. Li
CAS Key Laboratory of Organic Solids, Beijing National Laboratory for Molecular Sciences (BNLMS), CAS Research/Education Center for Excellence in Molecular Sciences, Institute of Chemistry, Chinese Academy of Sciences
Beijing 100190 (P. R. China)
E-mail: liuhb@iccas.as.cn
[b] J. Guo, F. Wang, W. Jin, Prof. H. Liu, Prof. Y. Li
University of Chinese Academy of Sciences
Beijing 100049 (P. R. China)
[c] M. Guo, Prof. C. Chen
CAS Key Laboratory for Biomedical Effects of Nanomaterials and Nanosafety and CAS Center for Excellence in Nanoscience, National Center for Nanoscience and Technology
Beijing 100190 (P. R. China)

Supporting information for this article is given via a link at the end of the document.

10.1002/anie.202006891

precursor GDY with larger size region ranging from 30 nm to 50 nm was exhibited in Figure S1. Figure 1c shows the high-resolution TEM (HRTEM) image of an individual GDY-Py flake. The defined interlayer distance of 0.36 nm is consistent with the previously reports.[11] Further, the distribution in size of the synthesized GDY-Py QDs was confirmed using dynamic light scattering (DLS) experiment. The volume-weighted DLS measurements confirm the small size of GDY-Py QDs (Figure 1d), showing a maximum of volume-weighted percent at ca. 3 nm with a size distribution between 1 and 18 nm. When irradiated with a red laser, the GDY-Py QDs solution presents a significant Tyndall phenomenon, indicating the uniform dispersion of GDY-Py QDs in dimethylformamide (DMF) (Figure 1d inset image).

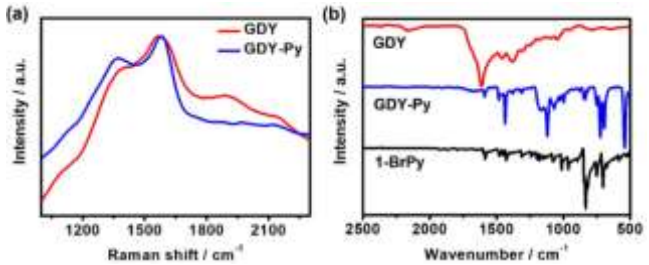

Figure 2. (a) Raman spectra of GDY and GDY-Py QDs. (b) FT-IR spectra of GDY, 1-BrPy, and GDY-Py QDs.

Raman spectroscopy was used to determine the quality of GDY (Figure 2a). There are two characteristic peaks at 1381.9 (D-band) and 1558.4 cm^{-1} (G-band). While D-band is assigned to the breathing vibration of sp^2 carbon domains in aromatic rings which is attributed to the disorder in the sp^2 hybridized carbon, the G-band is attributed to E_{2g} mode for in-phase stretching vibration observed for the sp^2 carbon lattice in aromatic rings.[12] Two weak peaks at about 1925.6 and 2143.1 cm^{-1} in the higher frequency region correspond to the vibration of conjugated diyne links (-C≡C-C≡C-).[13] After the functionalization with 1-BrPy, the D-band of GDY-Py QDs blue shifts to 1362.9 cm^{-1} and the G-band red shifts to 1578.5 cm^{-1}, evidence the attachment of 1-BrPy to GDY.[14] It was also noted that the D/G intensity ratio (I_D/I_G) increased from 0.82 in GDY to 0.93 in GDY-Py QDs, suggesting that the functionalization process induces 1-BrPy into the GDY structure to a higher sp^2 carbon defects density.[15] After modification, the increase of the conjugated system leads to the decrease of the electron cloud density of GDY-Py, which weakens the vibration of the diyne.

To demonstrate the bonding between 1-BrPy and GDY further, the Fourier Transform Infrared Spectra (FT-IR) of GDY, 1-BrPy, and GDY after 1-BrPy connection were compared in Figure 2b. FT-IR spectrum of GDY displayed absorption at 2162.1 cm^{-1} which is attributed to C≡C stretching vibration while the absorption bands at 1614.4 and 1458.1 cm^{-1} attributed to the skeletal vibrations of aromatic ring.[13] Two peaks at 1699.2 and 1665.1 cm^{-1} ascribable to the stretching vibration of C=O, due to the presence of oxygen in the form of carbonyl-groups and carboxyl-groups, respectively.[16] The absorption band at 1178.5 cm^{-1} is assigned to C-O stretching vibration.[17] Compared with GDY, many new peaks can be found in the FT-IR spectrum after modified with 1-BrPy. These new peaks at 400-1800 cm^{-1} are consistent with the FT-IR spectrum of pyrene groups, and appear with significant intensity, indicating that a large number of pyrene groups are connected to GDY.

Precursor GDY, 1-BrPy, and the synthesized GDY-Py QDs were then characterized by X-ray diffraction (XRD) and the diffraction patterns are shown in Figure S2. Precursor GDY exhibits a broad diffraction peak at 2θ values between 24° and 25° corresponding to the layer spacing of GDY at 0.36 nm, which is attributed to the (002) Bragg's reflection of graphite.[18] The well-defined peaks of 1-BrPy indicate high crystallinity of the pyrene crystal. The blue profile depicts the presence of GDY and 1-BrPy due to the attachment of the pyrene groups on GDY, which confirms the synthesis of GDY-Py QDs.

As shown in Figure 3a, GDY-Py QDs are soluble in both polar and nonpolar solvents. There is the highest solubility up to 1 mg/mL in THF. Figure 3b shows the UV-vis absorption spectra of 1-BrPy and GDY-Py QDs in tetrahydrofuran (THF). The absorption spectrum of 1-BrPy contains three strong bands whose intensity decreases slightly with the increase of wavelength in the range of 200 and 400 nm. The three bands can be assigned as ^1B_a transition (243 nm), ^1B_b transition (277 nm) and ^1L_a transition (345 nm) using Platt's nomenclature.[19] Compared with the absorption spectra of 1-BrPy, the absorption baseline of GDY-Py QDs is absorbed over the whole range, as expected by GDY dispersions. The presence of 1-BrPy on GDY is verified by the occurrence of characteristic peaks of 1-BrPy. Interestingly, GDY-Py QDs exhibit wider absorption peaks and higher absorbance compared to 1-BrPy, which may be due to the fact that 1-ByPy is attached to GDY and the conjugation effect enlarges the molar absorption coefficient in GDY-Py QDs.[20]

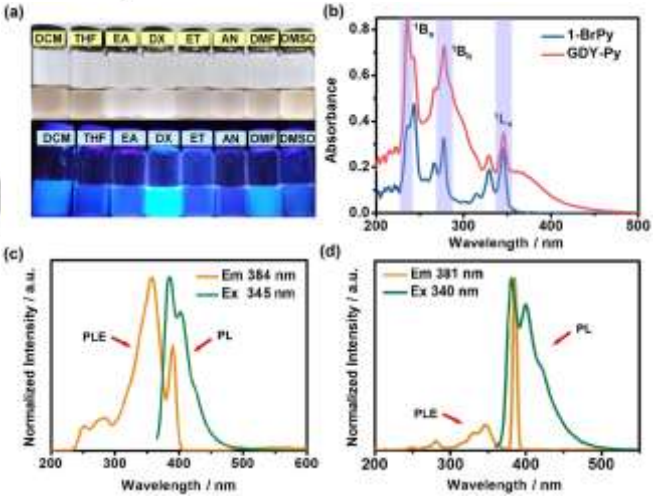

Figure 3. (a) Photographs of the 80 μg mL^{-1} GDY-Py QDs dispersions in dichloromethane (DCM), THF, ethyl acetate (EA), dioxane (DX), ethanol (ET), acetonitrile (AN), DMF, and DMSO from left to right and corresponding images under UV (365 nm) light. (b) UV-vis absorption of 1-BrPy and GDY-Py QDs in THF. (c) PLE and PL spectra of GDY-Py QDs in THF and (d) in a 50:1 H_2O/DMSO (v/v) solution.

Furthermore, the dispersion of the GDY-Py QDs in most solvents exhibits intense purple-blue fluorescence under UV light (Figure 3a) and the exhibited solvent-dependent PL behavior (figure S3) can be attributed to the different emission traps or solvent effects.[21] The photoluminescence excitation (PLE) spectrum with emission at 384 nm and photoluminescence (PL) spectrum excited at 345 nm of GDY-Py

10.1002/anie.202006891

QDs are obtained in THF solution at room temperature. As shown in Figure 3c, GDY-Py QDs shows emission bands associated with free pyrenes at 384 and 403 nm with no fine structure.[22] Figure S4 shows the representative PLE spectrum with emission at 379 nm and PL spectrum of 1-BrPy. Upon excitation at 345 nm, 1-BrPy exhibits two bands at 379 and 397 nm. It can be seen that compared with free 1-BrPy, the PL emission of the GDY-Py QDs red-shifted by about 5 nm (Figure S5). The red-shift in PL emission of the GDY-Py QDs indicated that the pyrenes were covalent band with GDY and the delocalization decreased the band gap.[23] Figures S6 are PL spectra of 1-BrPy and GDY-Py QDs at different excitation wavelengths, respectively. When the excitation wavelength changed from 236 nm to 345 nm, the emission wavelength of GDY-Py QDs almost unchanged except for the increase of intensity. Similarly, it was found that the intensity of emission peaks of 1-BrPy increased, but the two peaks remained at 379 and 397 nm without moving when excited from 243 to 345 nm.

The as-synthesized GDY-Py QDs can be used for cell imaging due to its wideband absorption and high fluorescence. The fluorescence experiments are carried out in a 50:1 H_2O/dimethyl sulfoxide (DMSO) (v/v) solution. The fluorescence properties of GDY-Py QDs H_2O/DMSO 50:1 solution are similar to those of THF solution: (1) The GDY-Py QDs H_2O/DMSO 50:1 solution shows two strong emission peaks at 381 and 400 nm upon excitation at 340 nm (Figure 3d). (2) The emission spectra of the GDY-Py QDs are excitation independent (Figure S7).

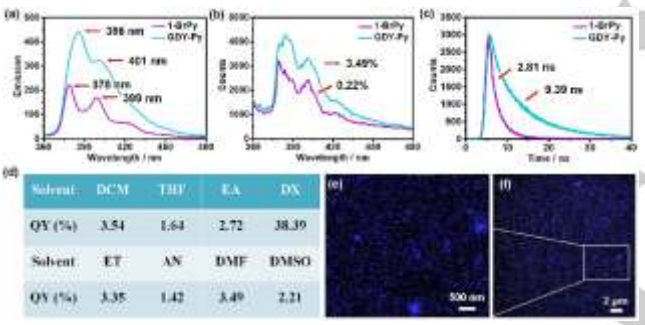

Figure 4. (a) Fluorescence spectroscopic changes and (b) absolute quantum yield of 1-BrPy and GDY-Py QDs in DMF, with the normalization of the absorbance at the excitation wavelength (347 nm) to the same value (0.2). (c) Fluorescence decays of 1-BrPy and GDY-Py QDs in DMF (excitation wavelengths of 360 nm and emission wavelengths of 386 nm). (d) The absolute quantum yield of GDY-Py QDs in different solvents, with the normalization of the absorbance at the excitation wavelength (347 nm) to the same value (0.2). (e, f) LCSM image and partial enlarged image of GDY-Py QDs.

Photophysical properties, including fluorescence emission, fluorescence lifetime (τ), and quantum yield, provide much information about the fluorescence behavior of GDY-Py QDs. As shown in the Figure 4a, when the absorption values of 1-BrPy and GDY-Py QDs at the excitation wavelength (347 nm) are equal to 0.2 (Figure S8), the maximum fluorescence emission peak of 1-BrPy was 378 nm, and a slight red shift was observed to 386 nm after the connection with GDY, which reflected the expansion of the conjugated system. We also observed an increase in the intensity of fluorescence emission for GDY-Py QDs compared with 1-BrPy. This phenomenon is partly explained by the increase of the delocalization region and the decrease of band gap caused by the conjugate connection between 1-BrPy and GDY. There are another two causes related to the red shift and enhancement of the emission peaks: (1) The tendency to form intermolecular aggregation may be reduced when 1-BrPy is connected at the edge of GDY, because extensive aggregation will lead to fluorescence quenching and blue shift.[24] (2) High light absorption efficiency due to the unique size of GDY-Py QDs, and the hyperchromic effect of UV-vis absorption is consistent with this mechanism.

The relative quantum yield of GDY-Py QDs was measured at 350 nm excitation and calculated to be 42.82% with quinine sulfate as a reference (Table S1) according to the following equation:[25]

$$QY_x = QY_R \times \frac{A_R}{A_x} \times \frac{I_x}{I_R} \times \frac{\eta_x^2}{\eta_R^2}$$

The fluorescence quantum yield of GDY-Py QDs was about 4.14 times higher than those of 1-BrPy (10.35%). To determine the absolute value of quantum yield, 1-BrPy and GDY-Py QDs were measured by photoluminescence spectrometer equipped with an integrating sphere detector. The absolute QY determined in DMF have been estimated with the value of 3.49% for GDY-Py QDs, which was higher than that of 1-BrPy, when excited at 347 nm (Figure 4b). To elucidate the effect of solvent polarity on the QY properties of GDY-Py QDs, absolute QY studies of GDY-Py QDs have been carried out in different solvents. As shown in Figure 4d, upon excitation at 347 nm with the normalization of the absorbance to the same value, the obtained GDY-Py QDs exhibit solvent-dependent QY behaviors.

The emission decay of 1-BrPy and GDY-Py QDs were also measured. The emission of 1-BrPy exhibits dual exponential decay as shown in Figure 4c. Therefore, the fluorescence decay profile (Table S2) of 1-BrPy was analyzed by biexponential function with a short lived one at 1.50 ns (74%) and a longer component at 4.15 ns (26%), in which the shorter lifetime (τ_1) is assigned to the excimer, and the longer lifetime (τ_2) is assigned to the monomer.[26] The intensity-weighted average lifetimes τ_m[27] of 1-BrPy derived from eqn. (1) is 2.81 ns.

$$\tau_m = \Sigma(a_i * \tau_i^2) / \Sigma(a_i * \tau_i) \quad (1)$$

where a_i is the percentage contribution of fitting and τ_i is the emission lifetime.

The emission lifetime decay of GDY-Py QDs can also be fitted by a double exponential function upon excited at 360 nm and monitored at 386 nm. Indeed, the biexponential emission lifetime of GDY-Py QDs at 3.49 ns (20%) and 9.91 ns (80%) is larger than that of 1-BrPy (Table S2), and τ_m of GDY-Py QDs is calculated to be 9.39 ns, more than three times that of 1-BrPy. Interestingly, we observed some differences in lifetime results obtained for GDY-Py QDs when compared to 1-BrPy. The percentage of the longer lifetime increased from 26% to 80%, while the percentage of the shorter lifetime decreased from 74% to 20% after the connection of pyrene with GDY. These changes could be related to the separation of pyrene molecules by GDY nanosheets and the high light absorption efficiency mentioned above. Besides, the electrons generated by GDY under illumination were transferred to pyrene through acetylene bonds at a rate faster than the dissipation rate, which supplemented the electrons needed for pyrene luminescence, thus making GDY-Py QDs has higher quantum yield and longer fluorescence life than 1-BrPy.

To further confirm the morphologies and optical properties of GDY-Py QDs, laser scanning confocal microscope (LCSM) imaging was performed on GDY-Py QDs dropped on a glass plate. Figure 4e and 4f show the representative LCSM images of GDY-Py QDs with a partially enlarged version, numerous purple-

blue fluorescent dots observed in the images are consistent with the observation in TEM. These results demonstrate good optical properties, which provide a direction for the application of this material in cell imaging.

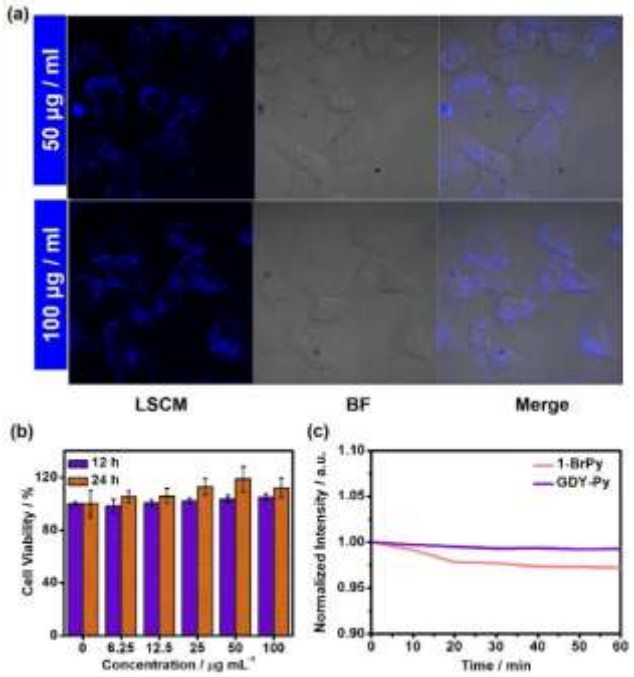

Figure 5. (a) Confocal fluorescence microscopy images, bright field (BF) images, and merge images of MDA-MB-231 cells cultured with GDY-Py QDs at 50 μg/mL and 100 μg/mL for 12 h at the emission wavelength of 405 nm. (b) Cell viability of MDA-MB-231 cells cultured with different concentrations of GDY-Py QDs for 12 and 24 h. (c) Stability tests of PL at 378 nm for 1-BrPy and 386 nm for GDY-Py QDs when excited at 347 nm.

As synthesized GDY-Py QDs excites at ca. 340 nm and emits at 380-400 nm, this feature will make it more suitable for biologically optical imaging. Figure 5a shows an array of cells incubated with GDY-Py QDs for 12 h. The blue fluorescence observed in MDA-MB-231 cells by LSCM indicated that GDY-Py QDs were taken up by the cells and the fluorescence intensity was depending on the concentration of GDY-Py QDs. The green color merged images indicate the colocalization of GDY-Py QDs with intercellular lysosomes (Figure S9). This result confirms that GDY-Py QDs are easily internalized by cells and the fluorescence property of GDY-Py QDs is a favorite for imaging.

Biological safety is a very important feature of the materials used as an imaging agent. To test the safety of GDY-Py QDs at the cell level, different concentrations of GDY-Py QDs were added into the culture medium of MDA-MB-231 cells and incubated for 12 h and 24 h. Figure 5b shows that GDY-Py QDs exposure had a negligible influence on cell viability up to 100 μg/mL, which suggests it could be a safe imaging agent. Furthermore, GDY-Py QDs exhibited slight photobleaching, whereas the fluorescence of 1-BrPy decreased significantly during continuous excitation at 347 nm for 60 mins (Figure 5c and Figure S10), indicating the outstanding photostability of GDY-Py QDs, which are essential for biological imaging.

In conclusion, GDY-Py QDs with strong fluorescence have been synthesized by Sonogashira cross-coupling reaction. The as-prepared GDY-Py QDs exhibits excellent dispersion in most organic solvents and water. The as-prepared GDY-Py QDs can be used to image cells, which effectively overcome the shortcomings of photobleaching of traditional fluorescent organic dyes. GDY-QDs display a high relative quantum yield of 42.82%, high stability, and long fluorescent time. The ideal biocompatibility, safety and long-term photostability of the newly designed graphdiyne QDs pave the path of a high-quality fluorescent probe to locate and monitor cells for biomedical applications.

Acknowledgements

This study was supported by the National Key Research and Development Project of China (2016YFA0200104, 2016YFA0201600), the National Nature Science Foundation of China (21875258, 21790050, 21790053), the Key Program of the Chinese Academy of Sciences (QYZDY-SSWSLH015).

Keywords: graphdiyne • chemical modification • quantum dot • quantum yield • cell imaging

[1] a) C. Huang, Y. Li, N. Wang, Y. Xue, Z. Zuo, H. Liu, Y. Li, *Chemical Reviews* **2018**, 118, 7744-7803; b) Y. Jiao, A. Du, M. Hankel, Z. Zhu, V. Rudolph, S. C. Smith, *Chem. Commun.* **2011**, 47, 11843-11845; c) X. Gao, J. Zhou, R. Du, Z. Xie, S. Deng, R. Liu, Z. Liu, J. Zhang, *Adv. Mater.* **2016**, 28, 168-173; d) L. M. Zhao, P. P. Sang, S. Guo, X. P. Liu, J. Li, H. Y. Zhu, W. Y. Guo, *Appl. Surf. Sci.* **2017**, 405, 455-464.

[2] a) C. Wang, P. Yu, S. Guo, L. Mao, H. Liu, Y. Li, *Chem. Commun.* **2016**, 52, 5629-5632; b) N. Parvin, Q. Jin, Y. Z. Wei, R. B. Yu, B. Zheng, L. Huang, Y. Zhang, L. H. Wang, H. Zhang, M. Y. Gao, H. J. Zhao, W. P. Hu, Y. L. Li, D. Wang, *Adv. Mater.* **2017**, 29, 1606755; c) H. Yan, S. Guo, F. Wu, P. Yu, H. Liu, Y. Li, L. Mao, *Angew. Chem. Int. Ed.* **2018**, 35, 3922-3926.

[3] H. Qi, P. Yu, Y. Wang, G. Han, H. Liu, Y. Yi, Y. Li, L. Mao, *J. Am. Chem. Soc.* **2015**, 137, 5260-5263.

[4] a) X. M. Qian, Z. Y. Ning, Y. L. Li, H. B. Liu, C. B. Ouyang, Q. Chen, Y. J. Li, *Dalton Trans.* **2012**, 41, 730-733; b) Z. Jia, Y. Li, Z. Zuo, H. Liu, C. Huang and Y. Li, *Acc. Chem. Res.* **2017**, 50, 2470-2478.

[5] a) C. Y. Kuang, G. Tang, T. G. Jiu, H. Yang, H. B. Liu, B. R. Li, W. N. Luo, X. D. Li, W. J. Zhang, F. S. Lu, J. F. Fang, Y. L. Li, *Nano Lett.* **2015**, 15, 2756-2762; b) H. Shang, Z. C. Zuo, L. Li, F. Wang, H. B. Liu, Y. J. Li, Y. L. Li, *Angew. Chem. Int. Ed.* **2018**, 57, 774-778; c) Z. C. Zuo, H. Shang, Y. H. Chen, J. F. Li, H. B. Liu, Y. J. Li, Y. L. Li, *Chem. Commun.* **2017**, 53, 8074-8077.

[6] T. Zheng, Y. Gao, X. Deng, H. Liu, J. Liu, R. Liu, J. Shao, Y. Li, L. Ji, *ACS Appl. Mater. Interfaces* **2018**, 10, 32946-32954.

[7] Y. H. Chen, J. F. Li, F. H. Wang, J. Guo, T. G. Jiu, H. B. Liu, Y. L. Li, *Nano Energy* **2019**, 64, 103932.

[8] D. Zhang, D. Liu, M. Li, Y. Yang, Y. Wang, H. Yin, J. Liu, B. Jia, X. Wu, *Anal. Chim. Acta* **2018**, 1033, 180-184.

[9] a) K. J. Mintz, Y. Zhou, R. M. Leblanc, *Nanoscale* **2019**, 11, 4634-4652; b) Z. Fan, S. Li, F. Yuan, L. Fan, *RSC Adv.* **2015**, 5, 19773-19789; c) C. Hu, M. Li, J. Qiu, Y.-P. Sun, *Chem. Soc. Rev.* **2019**, 48, 2315-2337; d) X. Wang, L. Cao, S.-T. Yang, F. Lu, M. J. Meziani, L. Tian, K. W. Sun, M. A. Bloodgood, Y.-P. Sun, *Angew. Chem. Int. Ed.* **2010**, 49, 5310-5314.

[10] Y. Niko, Y. Hiroshige, S. Kawauchi, G. I. Konishi, *Tetrahedron*, **2012**, 68, 6177-6185.

[11] a) X. Qian, H. Liu, C. Huang, S. Chen, L. Zhang, Y. Li, J. Wang, Y. Li, *Sci. Rep.* **2015**, 5, 7756; b) S. Zhang, H. Du, J. He, C. Huang, H. Liu, G. Cui, Y. Li, *ACS Appl. Mater. Interfaces* **2016**, 8, 8467-8473.

[12] a) F. Tuinstra, J. L. Koenig, *J. Chem. Phys.* **1970**, 53, 1126-1130; b) A. C. Ferrari, D. M. Basko, *Nat. Nanotechnol.* **2013**, 8, 235-246.

[13] G. Li, Y. Li, H. Liu, Y. Guo, Y. Li, D. Zhu, *Chem. Commun.* **2010**, 46, 3256-3258.

[14] A. D. Putri, N. Chotimah, S. K. Ujjain, S. Wang, R. Futamura, F. Vallejos-Burgos, F. Khoerunnisa, M. Morimoto, Z. Wang, Y. Hattori, T. Sakai, *Carbon* **2018**, 139, 512-521.

[15] D. Zaharie-Butucel, M. Potara, A. M. Craciun, R. Boukherroub, S. Szunerits, S. Astilean, *Phys. Chem. Chem. Phys.* **2017**, 19, 16038-16046.

[16] Y. Yao, Z. W. Jin, Y. H. Chen, Z. F. Gao, J. Q. Yan, H. B. Liu, J. Z. Wang, Y. L. Li, S. Z. Liu, *Carbon* **2018**, 19, 228-235.

[17] F. Zhao, N. Wang, M. Zhang, A. Sápi, J. Yu, X. W. Li, Z. Cui, Yang, C. Huang, *Chem. Commun.* **2018**, 54, 6004-6007.

[18] H. Bao, L. Wang, C. Li, J. Luo, *ACS Appl. Mater. Interfaces* **2019**, 11, 2717-2729.

[19] R.-S. Becker, I.-S. Singh, E. Jackson, *J. Chem. Phys.* **1963**, 38, 2144-

2171.
[20] I. Khalifa, R. Nie, Z. Ge, K. Li, C. Li, *Int. J. Biol. Macromol.* **2018**, 119, 116-124.
[21] a) D. Pan, J. Zhang, Z. Li, C. Wu, X. Yan, M. Wu, *Chem. Commun.* **2010**, 46, 3681-3683; b) D. Chen, W. Wu, Y. Yuan, Y. Zhou, Z. J. Wan, *Mater. Chem. C.* **2016**, 4, 9027-9035.
[22] a) Y. Kikuchi, H. Okamoto, T. Arai, K. Tokumaru, *Chem. Phys. Lett.* **1994**, 229, 564-570; b) M. Sharif, S. Reimann, K. Wittler, L. R. Knöpke, A.-E. Surkus, C. Roth, A. Villinger, R. Ludwig, P. Langer, *Eur. J. Org. Chem.* **2011**, 2011, 5261-5271.
[23] F. Liu, X. Shen, Y. Wu, L. Bai, H. Zhao, X. Ba, *Tetrahedron Lett.* **2016**, 57, 4157-4161.
[24] L. Ke, J. Min, M. Adam, N. Gasparini, Y. Hou, J. D. Perea, W. Chen, H. Zhang, S. Fladischer, A.-C. Sale, E. Spiecker, R. R. Tykwinski, C. J. Brabec, T. Ameri, *Adv. Energy Mater.* **2016**, 6, 1502355.
[25] S. Moonrinta, B. Kwon, I. In, S. Kladsomboon, W. Sajomsang, P. Paoprasert, *Opt. Mater.* **2018**, 81, 93-101.
[26] D. Zaharie-Butucel, M. Potara, A. M. Craciun, R. Boukherroub, S. Szunerits, S. Astilean, *Phys. Chem. Chem. Phys.* **2017**, 19, 16038-16046.
[27] L. Shang, L. Yang, H. Wang, G. U. Nienhaus, *Small* **2016**, 12, 868-873.

10.1002/anie.202006891

WILEY-VCH

COMMUNICATION

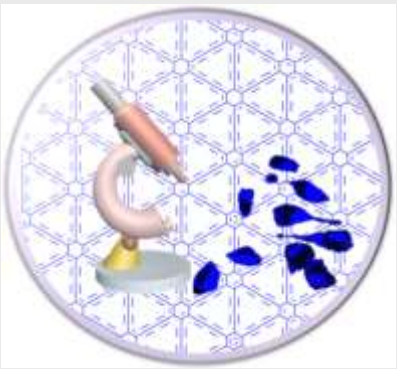

We develop a facile strategy to control the preparation of the graphdiyne quantum dots with high fluorescence quantum yield up to 42.82%, which exhibits superior dispersibility in many organic solvents and water. The excellent photophysical properties as well as the outstanding biocompatibility, safety and long-term photostability makes them offer great potential in optical imaging and biomedical application.

Jie Guo, Mengyu Guo, Fuhui Wang, Weiyue Jin, Chunying Chen, Huibiao Liu, Yuliang Li*

Page No. – Page No.

Graphdiyne : A New Structure of Fluorescent Quantum Dots